



University of Kurdistan

Dept. of Electrical and Computer Engineering

Smart/Micro Grid Research Center

smgrc.uok.ac.ir

Improvement of primary frequency control by inertial response coordination between wind and conventional power plants

S. Ataee, H. Bevrani

Published (to be published) in: *Intl trans. on Electrical Energy Systems*

publication date: **2017**

Citation format for published version:

S. Ataee, H. Bevrani. Improvement of primary frequency control by inertial response coordination between wind and conventional power plants. Intl trans. on Electrical Energy Systems. Vol(pp). Iss(pp). DOI: 10.1002/etep.2340. Mar, 2017.

Copyright policies:

- Download and print one copy of this material for the purpose of private study or research is permitted.
- Permission to further distributing the material for advertising or promotional purposes or use it for any profit-making activity or commercial gain, must be obtained from the main publisher.
- If you believe that this document breaches copyright please contact us at smgrc@uok.ac.ir providing details, and we will remove access to the work immediately and investigate your claim.

RESEARCH ARTICLE

Improvement of primary frequency control by inertial response coordination between wind and conventional power plants

Sirwan Atae¹  | Hassan Bevrani²

¹Electrical and Computer Engineering, University of Kurdistan, Sanandaj, the Islamic Republic of Iran

²Electical, University of Kurdistan, Sanandaj, the Islamic Republic of Iran

Correspondence

Sirwan Atae, Electrical and Computer Engineering, University of Kurdistan, Sanandaj, the Islamic Republic of Iran.

Email: sirwan.ataee@gmail.com

Summary

The constant increasing of wind power penetration leads to more and more retirement of conventional power generators. Since modern wind energy conversion machines are decoupled from the grid by the back-to-back voltage-based converters, they are not able to contribute to inertial response. Therefore, the reduced inertia of power systems at a high wind-power penetration level causes the greater rate of change of frequency following a power imbalance event and may bring the system to the crucial stability situation. In this study, the supported inertial response from the variable-speed wind turbines is based on electrically voltage-based converter control taken from stored kinetic energy of rotating mass of wind turbines. To enhance the frequency response, we proposed a new inertial coordination control between controlled wind turbines and conventional generators. So as to investigate the performance of the proposed method, we introduced a new primary frequency response metric. Also, a comparison between the effects of temporarily inertial support from wind farms and coordination of inertial support between wind and conventional power plants is done. The simulation results on an updated version of IEEE-39 bus power system in the presence of high penetration of wind farms indicate that by using the coordination control scheme, the frequency performance is significantly improved. The simulation is performed by MATLAB SimPowerSystems block set.

KEYWORDS

inertial control, inertial response, wind power penetration, coordination control, wind turbine

1 | INTRODUCTION

Power system reliability and stability need a system to maintain its electrical frequency within a safe range to a variety of contingencies.^{1–5} With the passing of the time, the distributed renewable energy source units replace a significant part of the synchronous power generation capacity, therefore the impacts of reduced inertia and damping on the frequency dynamics and stability become more and more considerable.^{2,3} Power industry tends to replace conventional generation units with the wind power resources in which leads to change in inertia and damping coefficient of the entire

system.^{3,4} Among distributed/renewable power generators, variable-speed wind turbines (VSWTs) such as doubly fed induction generator (DFIG) and permanent magnet synchronous systems gained more popularity in comparison with other power resources.^{6,7} The DFIG wind turbines do not have the capability to contribute in the frequency response. This is because the constraints are imposed by electronic-based voltage source converters. Therefore, the following reduced inertia and also the lack of primary frequency response (PFR) supporter can lead to system experience undesirable rate of change of frequency (RoCoF) and steady-state deviation from nominal frequency. Therefore, at high penetration of wind power, the combination of inertial and PFR of wind-power producers are more and more significant for the

*Senior Member, IEEE.

system reliability and stability point of view.⁴ Hence, recently, enhancement of the quality of primary frequency control of power system with high penetration of wind energy conversion system (WECS) has widely attracted the interest of system operators and many researchers. It is already shown that the inertial response and PFR support can be obtained from the VSWTs by imitating the role of conventional generators and consequently can improve the frequency response characteristics of the power system.^{7–13} However, the wind speed and curtailment condition can determine the amount of capability for providing extra energy and support from wind turbines for grid stabilization.¹⁴ To overcome the undesirable effect of reduced inertia and also the lack of PFR support, we find that the DFIG wind turbines can be equip with active power control loops.¹⁵

It is shown that,¹⁶ for a 2-MW DFIG, the amount of inertia of rotor is approximately 6 times than that of its electrical generator. Therefore, emulating inertial response and PFR response, which their energy extracted from rotor, can be sufficient to support the primary frequency control of the system.

The impact of using of extra control loops (which are sensitive to frequency response) on the PFR is investigated in the previous studies,^{17–20} and 1 study.¹⁴ In 1 study,¹³ the authors have investigate the impacts of participation of the demand side to the primary frequency control along with emulated inertial response from VSWTs and via implementing external control loops on the primary frequency control.

In addition to all aforementioned controllers, the deloded control can be assembled on the power converter of the VSWTs and consequently; can provide fast contribution of VSWTs in the primary frequency control. The important limitation for using these methods is the limitation of stored kinetic energy in the rotor of VSWT, which provides few seconds contribution in PFR of the power system.^{1,15,21,22}

In²³ articles the inertia constant and primary frequency reserve which can be provided by VSWTs are formulated. In the mentioned paper, the methodology is extended to estimate the availability of inertia support from wind farms in contingency events.

TABLE 1 List of nomenclatures and abbreviations

Nomenclatures	Abbreviations
Primary frequency response	PFR
Doubly fed induction generator	DFIG
Variable-speed wind turbine	VSWT
Renewable energy source	RES
Wind energy conversion system	WECS
Permanent magnet synchronous system	PMSG
Rate of change of frequency	RoCoF
Under frequency load shedding	UFLS
Maximum power point tracking	MPPT
Area control error	ACE
Automatic generation control	AGC
Instantaneous penetration	WP ₁

So far, a few studies have been concentrating on supervisory control level of wind farms with considering high penetration of these power resources.^{8,21,24,25} In 1 study,²⁴ only the coordination between provided PFR support from wind farms and conventional generators is investigated. In 1 study,²⁴ it has been shown that by this control mechanism, the conventional generators can accelerate their support for primary frequency control and relief secondary frequency control with better performance in frequency nadir value and steady-state performance. The major innovation of the present study is to analyze the impacts of new inertial coordination control between wind farms and selected set of automatic generation control (AGC)-controlled thermal power plants on the frequency response behavior (in the short-term frequency framework). In this new coordination mechanism, the thermal power plants are aware by system operator with the amount of inertial contribution of wind farms and will be alarmed to the conventional generators with the proper communication links. So, the received signal from wind farms modifies the AGC error, which is similar to the area control error signal. By implementing this control mechanism, a better performance in transient part of frequency response can be achieved rather than the wind farms inertial-only support from wind farms.

The rest of the study is summarized as follows: In Section 2, the proposed frequency performance metric and some other metrics are introduced. The details of the under study test system (New England test system) for implementation of simulations are given in Section 3. In Section 4, the description of proposed method for coordination of inertial control between wind farms and conventional generators is given. In Section 5, different wind penetrations for creating different scenarios are investigated to analyze the impacts of inertial control (with different strategies) on the primary frequency control. In Section 6, the results of emulating inertial response from wind farms and also coordination between wind farms and conventional generators are provided. At the end, the summarization of the study is given in Section 7. In addition, the list of nomenclatures and abbreviations are listed in Table 1.

2 | FREQUENCY RESPONSE METRIC

In Figure 1, a typical frequency response following a disturbance is shown. Some frequency response metrics are also depicted in this figure.^{25–27} In normal conditions, the system frequency will be kept close to the nominal frequency, which is predefined for the system. In Figure 1, point A represents the starting point for frequency response following a disturbance, point C indicates frequency nadir, which is influenced by the loss of kinetic energy in rotating mass of system, and point B represents the network frequency after governor response. Also, point D represents the steady-state frequency after 60 seconds of occurrence of disturbance. The value of

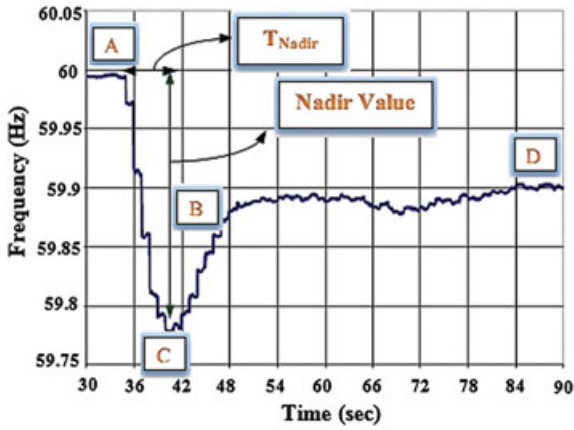


FIGURE 1 Description of frequency response metrics

point C can be influenced directly by the inertial response and capability of PFR of power resources following a disturbance in the power system.²⁹

A new frequency metric based on the concepts of the frequency nadir and frequency nadir time that takes advantages of both of them simultaneously and provides new information can be described as follows:

$$CT_R = \frac{|Nadir\ value|}{T_{Nadir}} \quad (1)$$

where, the $|Nadir\ value|$ is the absolute value of frequency nadir, and T_{Nadir} is the transition time from occurrence of disturbance to the frequency nadir. Since the frequency nadir depends on the total inertia of the system and also the capability of the power resources to provide PFR, the proposed metric can be dedicated to the assessment of improvement in short-term frequency response behavior caused by improvement in total inertia of the power system. So that, the frequency nadir shows the amounts of loss of rotating mass of power system and the frequency nadir time indicates the RoCoF and the amount of time that the other power resources have to take part in the primary frequency control more effectively.

In summary, in addition to the CT_R index, the metrics used in this study to analyze the short-term frequency performance are as follows: value of maximum drop of frequency (point C), the frequency settling value (point D), transition time between the 2 points; points A and C (T_{Nadir}), and

finally, the ratio of difference between points A and C to the difference between points A and D, which is known as the CB_R metric.^{28,29}

3 | PROPOSED CONTROL FRAMEWORK

The significant objective of this study is to study the impacts of inertial coordination control between wind and conventional power plants, using the aforementioned performance metrics, on the short-term frequency performance. Therefore, at each wind-power penetration level, the VSWTs (DFIG-based wind turbines) are equipped with fast injection of inertial response by adding control loops, which are sensitive to RoCoF.

3.1 | Wind turbine inertial control

The inertial control loops are equipped with dead-band, which has 2 main characteristics. (1) Preventing from activation of inertial response when it is not needed and (2) avoiding reduction of the machine lifetime¹⁴ (see Figure 2).

In this study, the inertial response boundary is chosen in a way that its margin safe from both system stability and reliability point of view. It is noteworthy that different power systems with different characteristics may have different values for their inertial response dead-bands.

It is shown that wind turbines can provide 0.1 pu extra active power support from their nominal value for 10 second quite easy.²⁸ Therefore, in this study, the tuned gain for $K_{Inertia}$ is obtained in a way that the wind turbine injects extra power (maximum power peak) about 10% of the actual output active power for the few seconds after occurrence of disturbance. In this study, the reference system frequency for the under consideration test system is considered 60 Hz.

Also, it is noteworthy that the reference value for reactive power of the contributed DFIG wind turbines in primary frequency regulation is set to 0.

3.1.1 | The impacts of wind turbines control parameters on the frequency response

The so-called inertia control adds terms to the output power reference (P_f) of the WECSs to be followed by WECS

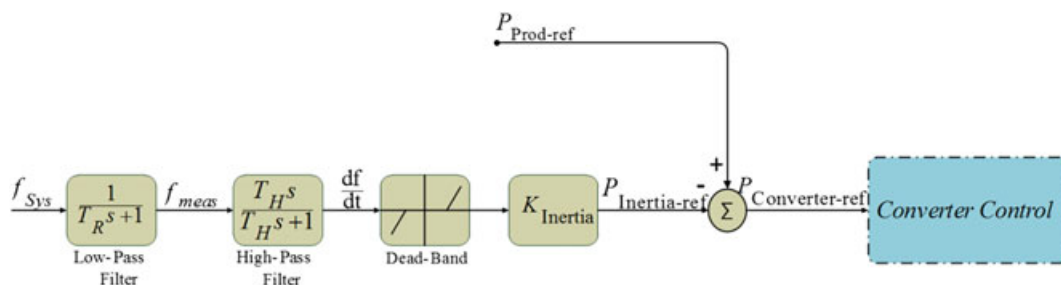


FIGURE 2 Structure of control strategy for DFIG-based wind turbine. DFIG, doubly fed induction generator

equivalent controller.^{10–12,14–18,21} The mentioned signal is obtained and demonstrates as follows:

$$P_f = -K_{\text{Inertia}} \frac{d\Delta f}{dt} - K_{\text{PFR}} \Delta f \quad (2)$$

where K_{Inertia} is a constant weight for the RoCoF deviation. In Equation 1, the term Δf is the frequency deviation, which measures behind high-pass filter; therefore, the continual frequency deviation can be eliminated and has no impact on the control strategy. Also, WECS limits and communication delay are taken into account for simulation purposes.

In this context, the equivalent WECS obtained their optimal speed once the frequency deviation is over. For this purpose, a power reference, forcing the speed to track a desire speed reference, is obtained as follows:

$$P_w^* = K_p (w_c^* - w_e) + K_I \int (w_c^* - w_e) dt \quad (3)$$

where w_e is the desired value for rotor speed of WECSs, K_p and K_I are the obtained constants of the Proportional Integrator (PI) controller of the speed control of the rotor of the unconventional generators, which must be determined.

Considering Equations 1 and 2, the total active power reference for WECSs is obtained as follows:

$$p_{fw}^* = p_f^* - P_w^* \quad (4)$$

The inherent characteristic of frequency transient for being in a short period causes simplification to be made. Basically, since p_w^* is obtained by a relatively slow PI controller, it would be reasonable that it can be assumed to be constant in a few seconds. In addition, as the electric power of WECSs is regulated by very fast power electronic converters, therefore, it can be assumed that the dynamic between power reference p_f^* and be nonconventional total power injection p_{NC} is eligible. This simplification results in

$$P_{NC} = P_f^* - P_{NC}^0 \quad (5)$$

where P_{NC}^0 is the injected power before occurring disturbance in the system frequency.

To analyze the impact of inertial response on the entire system, we find that the model can be considered as indicated in Figure 3, where P_L is the total active power demand and P_T is the total active power, which will exchanged with

neighboring system. On the basis of aforementioned equations, the relation between frequency deviation Δf and the power summation P_A can be obtained as follows:

$$2H \frac{d\Delta f}{dt} = P_A - D\Delta f = P_G + P_{NC} + P_T - P_L - D\Delta f \quad (6)$$

Then, by looking in-depth of Equation 4, the power P_{NC} as the following expression is obtained:

$$\underbrace{(2H + K_{\text{Inertia}})}_{2H^*} \frac{d\Delta f}{dt} = P_G + P_{NC}^0 + P_T - P_L - \underbrace{(K_{\text{PFR}} + D)}_{D^*} \Delta f \quad (7)$$

Therefore, the participation of nonconventional power sources in inertial response can be demonstrated in H^* . Variation in K_{Inertia} has impacts on H^* , so that positive value for the obtained gain (K_{Inertia}) increases the total inertia of the power system.

The shortcoming of inertial control is related to the fact that it is not considered as an inherent characteristic for nonconventional generator as considered for conventional power generators, like the fast active power response. In spite of injecting inertia to the entire system (from nonconventional power generators), this response is not direct, but may mask load change in the first few seconds.

3.2 | Wind-conventional power coordination scheme

The secondary frequency control provided by the AGC unit acts after primary frequency regulation of the power resources that is considered for restoring the frequency to the reference value.¹

With the participation of VSWTs in the inertial response, the inertia of entire system may mask the load change at the first few seconds of the load imbalance as a result of a considerable released inertia from the rotating mass of wind turbines although this support may lead to a delay in the output active power response of conventional power plants while attempting to contribute in frequency regulation.²¹

To resolve this issue, as shown is Figure 4, the AGC-controlled conventional power plants must be immediately aware of the amounts of the frequency support from wind farms. The provided inertial support from the VSWTs may be sufficient to enhance the system's frequency stability. However, using wind and conventional power coordination control, a better frequency behavior can be achieved as shown later. Here, a new control strategy is proposed so that the

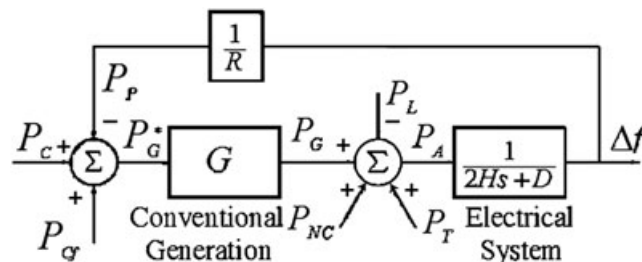


FIGURE 3 Power system model with presence of nonconventional generators¹⁹

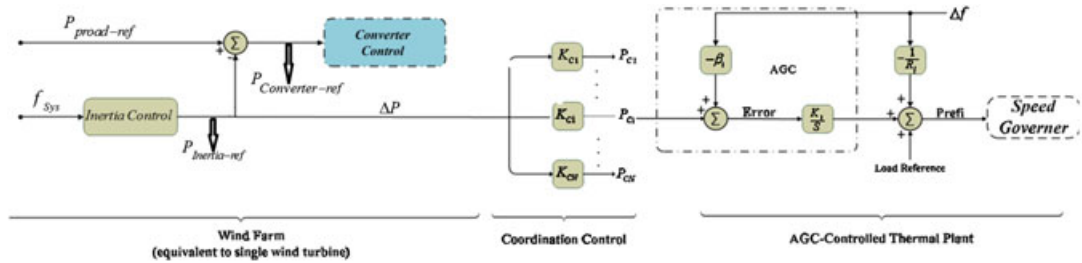


FIGURE 4 Proposed control scheme for wind-conventional power plant

output of individual wind farms control (inertial control) loop is coordinated with a selected AGC-controlled conventional power plant through proper communication links. The supporting power ΔP from wind farms is considered to provide the coordination control signal as follows:

$$P_{ci} = K_{ci}\Delta P \tag{8}$$

$$\sum_i K_{ci} = 1 \tag{9}$$

where, P_{ci} is the coordination control signal, K_{ci} is the participation factor for the i th selected conventional generator that considered for coordination control.

As shown in Figure 4, similar to the area control error signal, the amount of additional support from wind farms (P_{ci}) is added to the power reference of the synchronous generator. The wind-conventional inertial coordination control is based on the same principle as the tie line bias control. However,

the AGC error uses the coordination control signal P_{ci} instead of the tie line power deviation. Using this control strategy, conventional power plants realize the actual magnitude of RoCoF of the system since the very beginning and start their support to take part in inertial response of the system, more effectively. The flowchart of the control strategy as the main objective of the problem is shown below in Figure 6.

4 | NEW ENGLAND TEST SYSTEM

New England system is a well-known test system that is widely used as a standard system for testing of power system analysis and control methodologies. In this study, the great reduced version of New England test system is used with the same topology. The system has 12 transformers, 10 generators, 34 transmission lines, and 19 loads and this test system includes 3 interconnected areas, which its data are given in 1 study.²⁷ The total system capacity is 886.54 MW of conventional

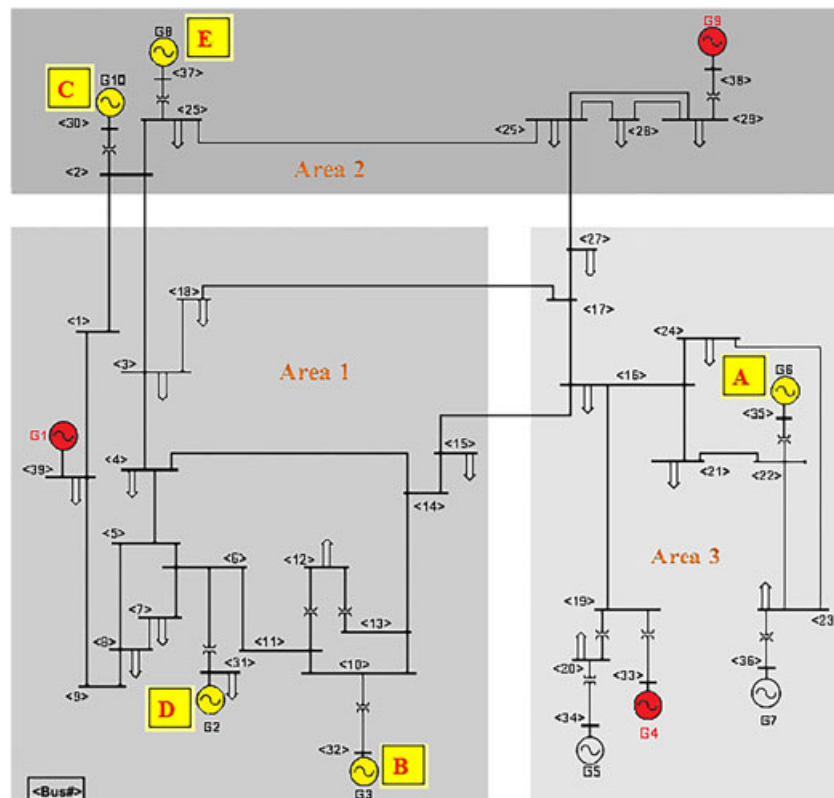


FIGURE 5 Single diagram of New England test system

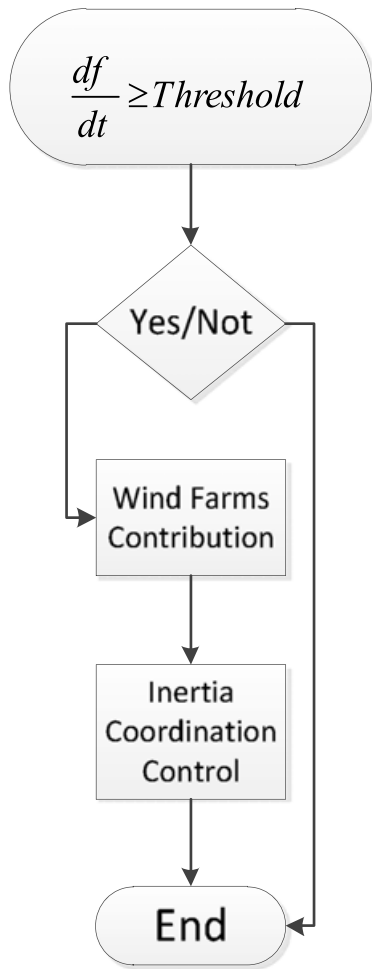


FIGURE 6 Flowchart of the control procedure

generation. There are 221.63 MW of conventional generation and 265.25 MW of load in area 1. Area 2 consist of 232.83 MW of conventional generation and 232.83 MW of load. Also in area 3, there are 183.17 MW of conventional generation and 124.78 MW of load.

The system includes 10 thermal conventional power plants with steam-turbine governor that are equipped with power system stabilizers and speed governors. The generators are represented using their fifth-order models extended by IEEE-type excitation and governor models. For being similar to real power systems, in the simulations scenarios, the important inherent requirement and basic constraints such as generation rate constraint and governor dead-band that imposed by system dynamic and characteristic are considered.

A single-line diagram of the test system is shown in Figure 5. The letters A to E in the diagram indicate the points that the conventional power plants to be replaced by the wind generators.

5 | SCENARIO DEVELOPMENT

As previously mentioned, the outstanding objective of this study is to assess the impacts of proposed coordinated inertial control between conventional power plants and wind on the

short-term frequency performance of power system considering high levels of wind power penetration. For this purpose, some of the DFIG wind turbines, which equipped with fast primary frequency regulation, are replaced with a few number of conventional power plants which the replacement point and overall share of wind power in the test system are staggered incrementally as shown in Table 2.

The overall share of wind generation at Point A is 9.3% in relation with the overall load in the system. Impact of each addition, starting from Point B (20% wind power penetration) to all others up to Point E (50% wind power penetration) has been studied separately.

In the present work, the definition of wind power penetration is considered as the ratio of the present wind power production to the present system load, which is known as instantaneous penetration (WP_1):

$$WP_1 = \frac{\text{Actual Wind Power Production (MW)}}{\text{Actual System Load (MW)}} \quad (10)$$

It is noteworthy that the wind turbines in this study are operating at 13 m/s wind speed that assumed to be constant, while the rated wind speeds for all of the DFIG wind turbines are specified at 14 m/s. By considering the short-term framework for simulations (tens of seconds) in this work, this assumption is reasonable. In the aforementioned scenarios, to show the worst load increment that may happen, 2 steps load increment about 10% of total area load, are simultaneously applied to the 3 areas at 5 seconds. The amounts of load increment in 3 areas are considered great enough to simulate considerable loss of kinetic energy in the test system. In the last scenario, the generator 7 will be tripped to study the coordinated inertia scheme under severe wind speed fluctuations.

6 | SIMULATION RESULTS AND DISCUSSION

The applied control strategies for all wind penetration levels are summarized in Table 3. As shown in Table 4, for the

TABLE 2 Wind power penetrations and scenarios

Point of Connection	B	C	D	E
Overall share of wind generation, %	20	30	40	50
Wind generation, MW	118	186.858	294.144	311.43
Scenarios	1	2	3	4

TABLE 3 The summary of simulation scenarios

Scenarios And Penetration Levels (%)	Control Strategies		
Scenario 1 (20%)	No control	Inertia support from wind farms	Coordinated inertia support
Scenario 2 (30%)			
Scenario 3 (40%)			
Scenario 4 (50%)			

TABLE 4 Selected conventional generator for coordination control

Generator Unit	Rated Power, MVA	Participation Factor
G1	150	0.42
G9	120	0.34
G4	85	0.24

coordination control between wind and power plants, only 1 conventional power plant is considered in each area; G1 in area 1, G9 in area 2, and G4 in area 3. These generators are selected on the basis of greatest apparent power in each area. Therefore, the generator with greatest apparent power allocates the biggest participation factor among the mentioned selected generators. The amounts of power reserves for effective contribution of selected generators in the primary frequency control are considered.

In Table 5, the numerical details associated with wind turbine inertial control loop (Figure 2) and for one of the wind farms in Scenario 1 are provided. These parameters may vary in different scenarios. In this work, these parameters are adjusted by simulation in an iterative procedure.

Figures 7–10 show the performed simulated frequency response for 4 wind power penetration scenarios and different strategies for inertial response participation of unconventional power plants such as the following: no control support from wind farms (blue trace), inertial support from wind farms (green trace- $Inertia_W$), and coordination control between inertial support from wind farms and conventional generators (black trace- $Inertia_C$).

In Figures 7–10, the decline of the nadir frequency for no control support strategy (blue traces) is caused by the lack of inertial response from wind power, which are replaced with the supportive conventional generation. So, the frequency response for no control strategies has fallen below the considered under frequency load shedding (UFLS) threshold for 40% and 50% of wind penetrations. Therefore, the contribution of uncontrolled power resources seems more necessary in these levels of penetrations. As wind power penetration enhances, the effective of the control strategies would be more and more outstanding.

Frequency nadir is dependent on the stored kinetic energy in rotor of the available machine in the system, the number of the generators which contribute in PFR, the system dynamic and the type and magnitude of disturbance, and finally the characteristic of the power network.^{2,25} As shown in Figures 6–9, the inertial response from wind farms (green trace) has had outstanding enhancement on the frequency nadir of higher levels of wind penetration (Figure 10) in comparison with the lower penetrations (Figures 7–9) in each penetration. This issue is due to the more installed unconventional power generators with the capability in contributing in

TABLE 5 Details of inertial control parameters in Scenario 1

Parameter	T_R	T_H	Dead-Band	$K_{Inertia}$
Value	0.1 s	0.15 s	± 0.04	0.85

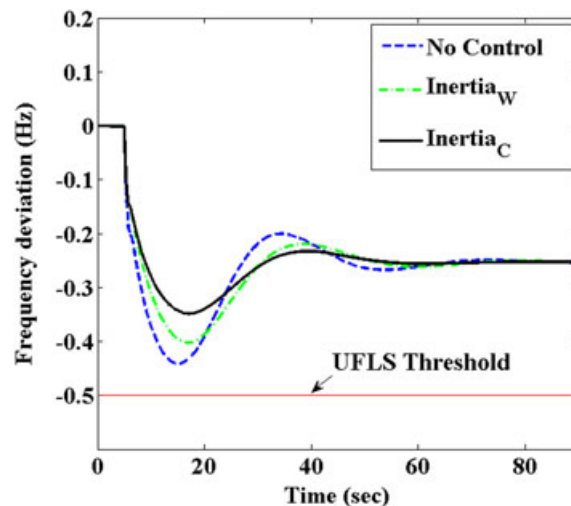


FIGURE 7 Frequency response for Scenario 1 (20% wind power penetration)

frequency regulation (power supporters) in comparison with lower penetrations. By providing inertial control support from wind farms, the transition time to frequency nadir increased with increment in wind penetration levels, so other conventional power resources obtain more time to contribute in PFR more effectively. Moreover, by providing the inertial support from wind farms ($Inertia_W$), the greatest improvement is seen at 50% wind power penetration in which frequency nadir value is improved from -0.7842 (no control support) to -0.5557 Hz. The lowest improvement is seen in Scenario 1 (see Figure 7), because of the lower amount of inertial response from installed DFIG-based wind farms, which improved the frequency nadir from -0.4413 (no control support) to -0.4025 Hz (inertial support from wind farms).

On the other hand, with the coordinated inertial control (black trace- $Inertia_C$), the nadir value and transition time to frequency nadir are improved significantly in comparison with provided inertial control support from wind farms. The further enhancement in frequency nadir time is due to additionally provided inertial support from coordinated conventional

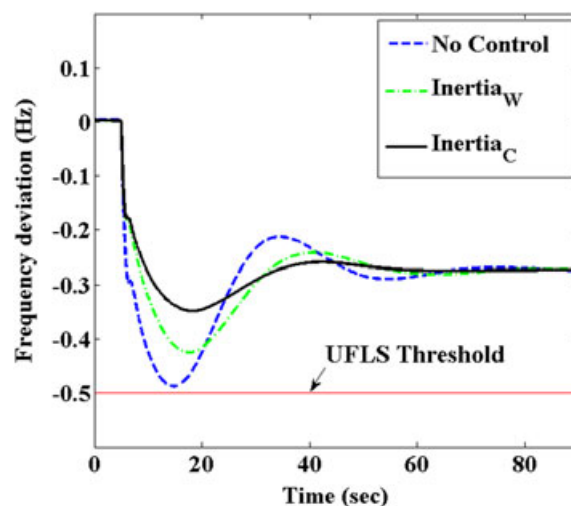


FIGURE 8 Frequency response for Scenario 2 (30% wind power penetration)

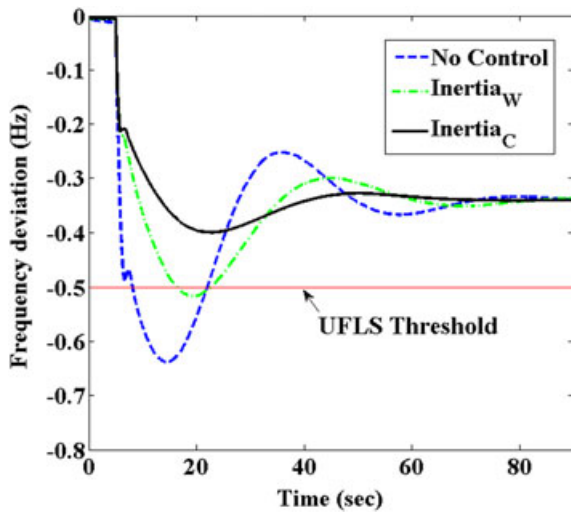


FIGURE 9 Frequency response for Scenario 3 (40% wind power penetration)

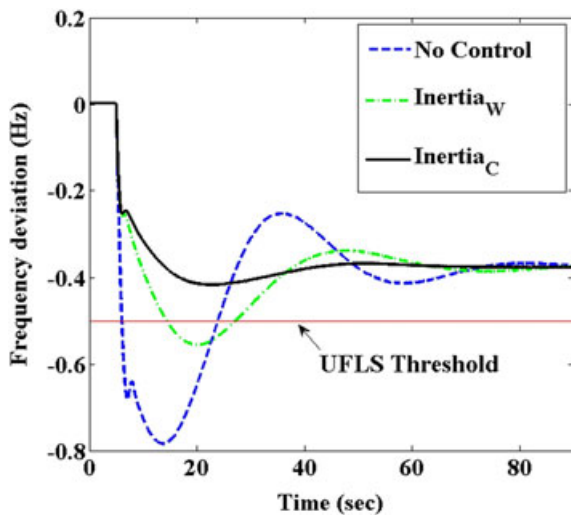


FIGURE 10 Frequency response for Scenario 4 (50% wind power penetration)

control structure. The more available inertial support, the more decrease in RoCoF. Therefore, conventional generators have more time to effectively participate in the primary frequency control that leads to more improvement in frequency nadir.

For example, by applying the coordinated inertial support, the frequency nadir at 50% wind penetration level is improved from -0.7842 (for no control support) to -0.4169 Hz (for coordinated inertial support). With further investigation of Figures 8, 9, and 10, the superior performance of the proposed control is illustrated, so that with the wind farms-only contribution to the inertial response, the frequency nadir is still below UFLS threshold; however, by implementing coordinated inertial control, the value of frequency nadir is apparently enhanced above the specified UFLS threshold.

Figure 11 shows the frequency nadir deviation for all performed scenarios and all wind penetration levels. The coordinated inertial control has had the best improvement in frequency nadir at any penetration levels than other control

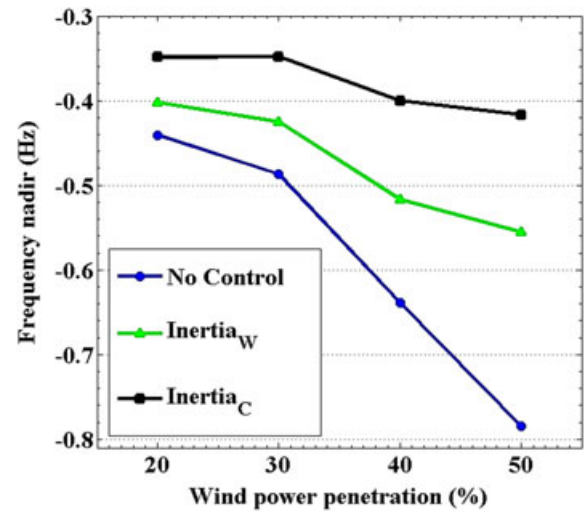


FIGURE 11 Impact of wind power contribution on the frequency nadir

strategies. The effectiveness of the proposed coordination control has more and more resolution with increment in wind power penetration level. So that for the coordination control, the absolute values of improvement of the frequency nadir from no control strategies are 0.0927, 0.1391, 0.2383, and 0.3673 for Scenario 1 to Scenario 4, respectively. Further analysis of Figure 11 shows that the supported inertia-only from wind farms cannot bring the frequency nadir above UFLS setting for the test system at penetrations greater than 30%; however, with the coordination control, in any penetration, the frequency nadir is extensively above the highest considered UFLS threshold especially at 50% penetration.

In Figure 12, the frequency nadir time for all of the control strategies is shown. Without any control support (blue trace), the nadir time decreased with increment in wind power penetration while on the contrary by enabling the wind farms to contribute to inertial response (green trace- $Inertia_W$), the nadir time significantly increased with the increment in penetration levels. Therefore, the greatest improvement is seen in Scenario 4 (50% wind power penetration) in which the nadir

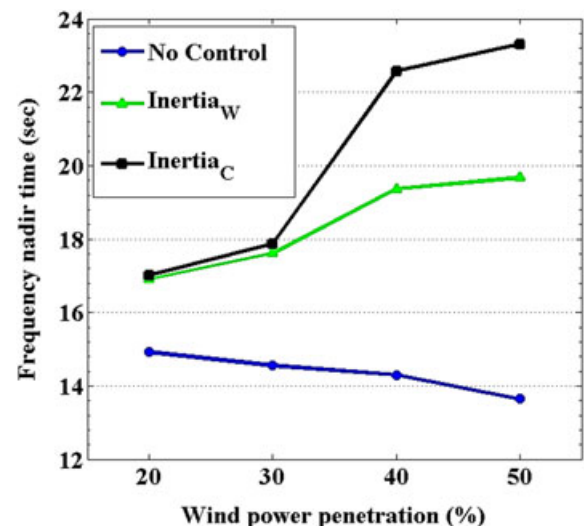


FIGURE 12 Impact of wind power contribution on the frequency nadir time

time is improved from 13.65 (for no control support) to 19.67 seconds. As shown in Figure 11, the superior improvement in nadir time is obtained by applying the coordinated inertial control (black trace-Inertia_C). Similar to contribution of wind farms in inertial response, the effectiveness of the proposed control is more obvious with the increment in wind power penetration levels because of further inertial support, and therefore, more declining in RoCoF at higher penetration levels. With the coordination control, the greatest improvement in the nadir time is seen in Scenario 4 (50% wind power penetration) in which the nadir time is increased from 13.65 (for no control support) to 23.31 seconds. In Table 6, the CB_R performance metric for without control support strategy (column 2), inertial control support from wind farms (column 3), and coordinated inertial support (column 4) is calculated for all of the wind penetration levels.

In 1 study,⁴ where the wind farms are participated in PFR support effectively, the attitude of CB_R for improvement is determined with the increment in its value. However, in the present work, because of the focus on the inertial response support from VSWTs (the absence of PFR support), the settling frequency remained nearly constant at each scenario. Therefore, in our study, contrary to another study,⁴ the improvement in CB_R is determined with decrease in its value. Therefore, the improvement in CB_R value increased with the increment in penetration level (columns 3 and 4).

So that the best CB_R metric is calculated for coordinated inertial support at 50% wind power penetration (Scenario 4) that improves the value of this metric from 2.08 (the worst value of CB_R for no control strategy) to 1.107 (the best value of Table 6).

In Table 7, the proposed performance metric for no control support (column 2), inertial control support from wind farms (column 3), and coordinated inertial support (column 4) is calculated.

TABLE 6 Impact of wind farms control on the CB_R frequency performance metric

Scenarios And Penetration levels (%)	CB _R No Control	CB _R Inertia Support From Wind Farms	CB _R Coordinated Inertia Support
Scenario 1 (20%)	1.744	1.590	1.377
Scenario 2 (30%)	1.783	1.556	1.274
Scenario 3 (40%)	1.891	1.531	1.185
Scenario 4 (50%)	2.08	1.476	1.107

TABLE 7 Impact of wind farms control on the CT_R frequency performance metric

Scenarios And Penetration levels (%)	CT _R No Control	CT _R Inertia Support From Wind Farms	CT _R Coordinated Inertia Support
Scenario 1 (20%)	0.029578	0.023802	0.020505
Scenario 2 (30%)	0.033490	0.024145	0.019485
Scenario 3 (40%)	0.044636	0.026699	0.017723
Scenario 4 (50%)	0.057451	0.028251	0.017885

The frequency nadir in power systems is determined by the total system inertia (rotating mass in the system) and the capability of providing PFR of power resources following a disturbance in the power system, while, the nadir time depends on the inertial response of the power system. On the other word, the nadir time extensively depends on the RoCoF. So, enhancement in the total inertia of power system by contributing the wind farms in inertial response leads to particularly improvement in CT_R metric that implies improvement in major indices of inertial response of power system such as frequency nadir and frequency nadir time, simultaneously.

The improvement in CT_R metric is determined with the decrease in its value. As indicated in Table 7, the value of this metric is worsted when the wind penetration level is increased for no control support approach, (column 2) so that the greatest value is obtained at 50% of wind penetration (Scenario 4), because with the increment in power penetration the nadir time remained in a close range but the frequency nadir decreased extensively. By enabling the wind farms to participate in the inertial response, the value of this metric decreased with the increment in wind power penetration significantly (column 3) so that, the most improvement in this metric is obtained for Scenario 4 where the metric's value is improved from 0.057451 (for no control) to 0.028251. The superior improvement in CT_R metric is obtained by applying the inertial coordination control between wind farms and conventional power plants (column 4). Because of the further inertial response from contributed conventional generators in coordination control, the frequency nadir and nadir time are dramatically improved. The greatest improvement is seen in Scenario 4 where the CT_R value is improved from 0.057451 (for no control) to 0.017885. Also the lowest improvement belongs to Scenario 1 (20% wind power penetration) because of the fewer amounts of installed wind farms (and so lower amounts of emulated inertial response) in this scenario.

The output active power response of G1 in area 1 as the most effective participated generators is shown in Figures 13 and 14. It is apparent that the contributions of wind farms in inertial response have had adverse impacts on the output active power response of generators (green trace-Inertia_W). The wind output active power of generators is delayed depending on the amount of released inertial response from the contributed wind farms. The impact of this phenomenon increased with the increment in wind power penetration levels (see Figure 14). By applying the coordination control (black trace-Inertia_C), the adverse impact of contribution of wind farms on the output active power response of generators, is eliminated, as the penetration increases the amplitude of the additional input power reference signal for the AGC-based conventional generators increases. Hence, the fastest active power support provided by the participated generators at 50% of wind penetration level (Figure 14).

In Figures 15 and 16, the RoCoF response of area 1 (as a sample) and for the 3 control strategies is shown. By

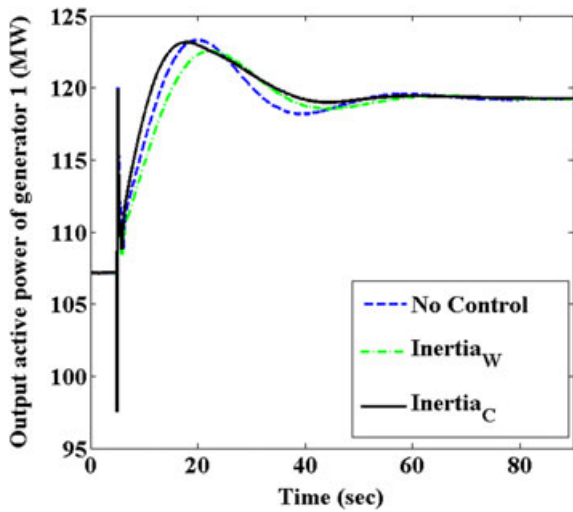


FIGURE 13 Output active power response of generator 1 for Scenario 1 (20% wind penetration)

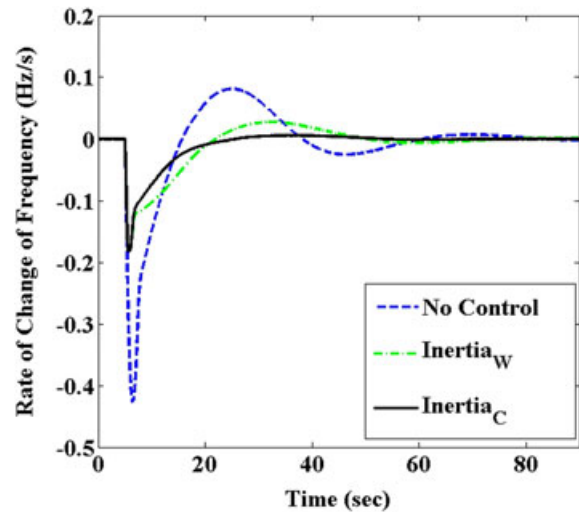


FIGURE 16 Rate of change of frequency response for Scenario 4 (50% wind penetration)

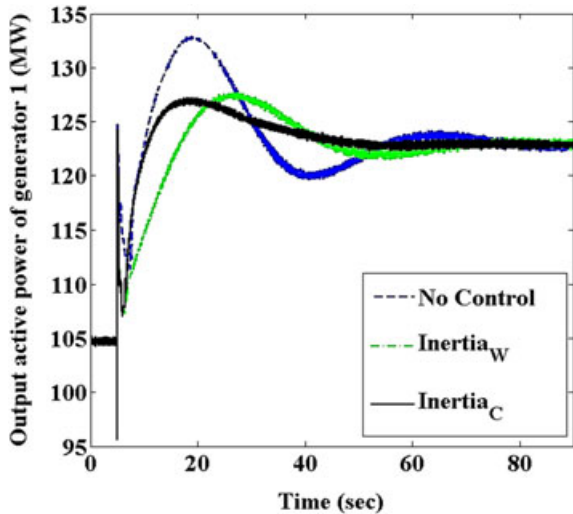


FIGURE 14 Output active power response of generator 1 for Scenario 4 (50% wind penetration)

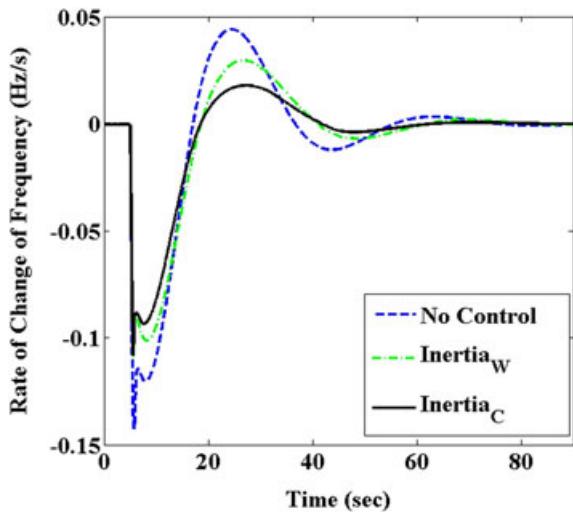


FIGURE 15 Rate of change of frequency response for Scenario (20% wind penetration)

providing inertial support from wind farms (green trace- $Inertia_W$) and inertial coordination support (black trace- $Inertia_C$), the amount of improvement in RoCoF in Scenario 1 (20% wind power penetration) does not have the same resolution of improvement compared to Scenario 4 (see Figure 15). In Figure 16, it is shown that at 50% penetration level, applying the coordination control causes more decrease in the RoCoF oscillations and therefore more smoothness in the RoCoF response in comparison with 20% penetration level (See Figure 16). More smoothness in RoCoF response means more improvement in frequency nadir time, so it can lead to provide more time for power resources of system to effectively participate in primary frequency regulation.

6.1 | Impact of wind speed fluctuation on the coordination control scheme

In this scenario, the coordinated control is examined under realistic condition (variation of wind speed).

For this purpose, the wind speed will be varied for ± 2 m/s. Instead of losing active load, tripping the generator 7 at second 5 is considered as the major fault in the system. The variation of wind speed for the 5 wind farms is illustrated in Figure 17.

The corresponding frequency response following the variation of wind speeds is shown in Figure 18. By further analysis of Figure 16, it is obvious that no support (black-trace) strategy has lower performance in comparison with other strategies. The best result is obtained for coordinated inertial response (blue-trace). The green trace is corresponding to the provided inertial response from wind farms. It is noteworthy that for being more effective of coordination control, the absolute value of the provided signal from wind turbines external control loop is sent to conventional generators.

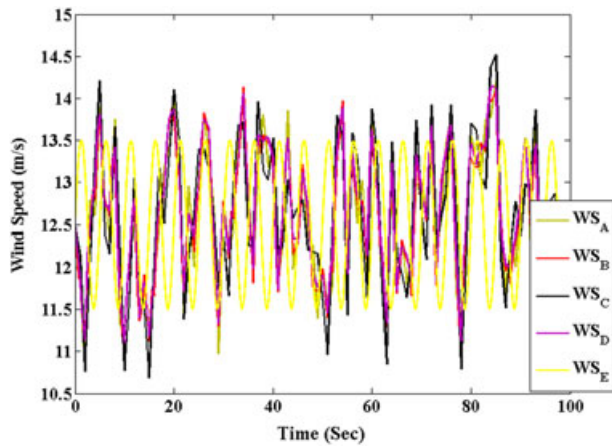


FIGURE 17 Wind speed fluctuation for installed wind turbines

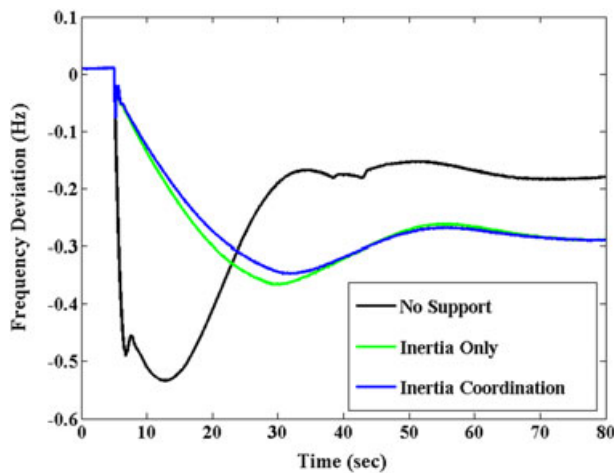


FIGURE 18 Frequency response for 50% wind power penetration

7 | CONCLUSION

This study introduced a new coordination scheme between wind farms and conventional generators. Several simulation scenarios and wind power penetration levels on reduced model of IEEE 39-bus system are performed to assess the PFR performance, which is caused by load increment in each area of 3 interconnected areas of the test system. It is shown that the coordination control strategy approach has outstanding improvement in frequency response performance in each penetration level. Simulation results show that provided inertia only from wind farms can improve the frequency response performance but in higher penetration of wind power, this support may not be sufficient so the new inertia control strategy introduced to overcome the mentioned problem. The coordinated inertial control had significant impact on PFR in each level especially at high penetration levels so that the greatest improvement is observed for 50% wind power penetration. On the other hand, the least enhancement are shown in lowest wind power penetration level (20% penetration), because in lower wind penetration there are fewer number of (equipped with fast primary control support) wind farms

in the power system. The impact of coordinated control strategy is investigated on the output active power of conventional generated. It is shown that in spite of increasing the speed of governor response in this control strategy, leads to delay in output active power of conventional generators.

Also, the variable wind speed is applied for wind farms to examine the proposed coordination control in real condition. In this condition, the applied fault was tripping of one of the major conventional generators, and the simulation results show the remarkable capability of the proposed control strategy.

In this study, a new performance metric (CT_R) is introduced. As mentioned previously, this new metric reflect the attitude of the nadir value and nadir time simultaneously to determine the amount of improvement in inertial control of frequency response. The best value (the lowest value) for this metric was obtained for coordination control strategy at the highest wind power penetration.

REFERENCE

1. Bevrani H. *Robust Power System Frequency Control*. 2nd ed. NY: Springer; 2014.
2. Bevrani H, Ghosh A, Ledwich G. Renewable energy sources and frequency regulation: survey and new perspectives. *Renew Power Gener IET*. 2010;4(5):438–457.
3. Naik PK, Nair NKC, Swain AK. Impact of reduced inertia on transient stability of networks with asynchronous generation. *Int Trans on Electr Energy Syst*. 2016;26(1):175–191.
4. Gevorgian V, Yingchen Z, Erik E. Investigating the impacts of wind generation participation in interconnection frequency response. *IEEE Trans Sustain Energ*. 2015;6(3):1004–1012.
5. Abd-Elazim SM, Ali ES. Load frequency controller design via BAT algorithm for nonlinear interconnected power system. *Int'l J Electr Power & Energy Syst*. 2016;77:166–177.
6. Ahmadi R, Sheikholeslami A, Nabavi Niaki A, Ranjbar A. Dynamic participation of doubly fed induction generators in multi-control area load frequency control. *Int Trans on Electr Energy Syst*. 2015;25(7):1130–1147.
7. Ghosh S, Kamalasadnan S, Senroy N, Enslin J. Doubly fed induction generator (DFIG)-based wind farm control framework for primary frequency and inertial response application. *IEEE Trans on Power Syst*. 2016;31(3):1861–1871.
8. Ansari J, Mahdi J, Ahad K. Integration of the wind power plants through a novel, multi-objective control scheme under the normal and emergency conditions. *Int Trans on Electr Energy Syst*. 2016.
9. Chang-Chien L-R, Yin Y-C. Strategies for operating wind power in a similar manner of conventional power plant. *Energy Conversion IEEE Trans*. 2009;24(4):926–934.
10. Conroy JF, Watson R. Frequency response capability of full converter wind turbine generators in comparison to conventional generation. *Power Syst IEEE Trans*. 2008; [10] Ahmadi R, Sheikholeslami A23(2):649–656.
11. Nabavi Niaki A, Ranjbar A. Dynamic participation of doubly fed induction generators in multi-control area load frequency control. *Int Trans on Electr Energy Syst*. 2015 Jul 1;25(7):1130–1147.
12. Li S, Deng C, Chen L, Wu Z, Zheng F. A novel inertial control method suitable for doubly fed induction generator considering stability constraints. *Int Trans on Electr Energy Syst*. 2015 Dec 1;25(12):3630–3643.
13. Molina-García A, Muñoz-Benavente I, Hansen AD, Gómez-Lázaro E. Demand-side contribution to primary frequency control with wind farm auxiliary control. *IEEE Transactions on Power Systems*. 2014;29(5):2391–2399.
14. Margaris ID, Papathanassiou SA, Hatziargyriou ND, Hansen AD, Sorensen P. Frequency control in autonomous power systems with high wind power penetration. *Sustain Energ IEEE Trans*. 2012;3(2):189–199.

15. Xue Y, Tai N. System frequency regulation in doubly fed induction generators. *Int J Electr Power and Energ Syst*. 2012;43(1):977–983.
16. Tarnowski C. “Coordinated frequency control of wind turbines in power systems with high wind power penetration,” *PhD thesis, Technical University of Denmark*, 2012.
17. El Itani S, Annakkage UD, Joos G. “Short-term frequency support utilizing inertial response of DFIG wind turbines,” in *Power and Energy Society General Meeting, 2011 IEEE*, 2011, pp. 1–8.
18. Ramtharan G, Jenkins N, Ekanayake JB. Frequency support from doubly fed induction generator wind turbines. *IET Renew Power Gen*. 2007;1(1):3–9.
19. Wang-Hansen M, Josefsson R, Mehmedovic H. Frequency controlling wind power modeling of control strategies. *IEEE Trans on Sustainable Energy*. 2013;4(4):954–959.
20. Ali ES. Speed control of induction motor supplied by wind turbine via imperialist competitive algorithm. *Energy*. 2015;89:593–600.
21. Singhvi V, Pourbeik P, Bhatt N, Brooks D, Zhang Y, Gevorgian V, Ela E, Clark K. “Impact of wind active power control strategies on frequency response of an interconnection,” in *Power and Energy Society General Meeting (PES), 2013 IEEE*, 2013, pp. 1–5.
22. Ataee S, Khezri R, Feizi MR, Bevrani H. “Investigating the impacts of wind power contribution on the short-term frequency performance,” in *4rd Smart Grid Conference, (SGC), 2014*, vol., no., pp. 1-6, 9-10, Dec. 2014.
23. Ye H, Pei W, Qi Z. “Analytical Modeling of Inertial and Droop Responses From a Wind Farm for Short-Term Frequency Regulation in Power Systems.”
24. Mauricio JM, Marano A, Gómez-Expósito A, Martínez Ramo JL. Frequency regulation contribution through variable-speed wind energy conversion systems. *Power Syst IEEE Trans*. 2009;24(1):173–180.
25. Bevrani H, Hiyama T (Eds). *Intelligent a Utomatic Generation*. New York, NY: CRC Press (Taylor & Francis Group); 2011.
26. Lubosny Z, Bialek JW. Supervisory control of a wind farm. *Power Syst IEEE Trans*. 2007;22(3):985–994.
27. Bevrani H, Toshifumi I, Miura M. Virtual synchronous generators: a survey and new perspective. *International Journal of Electrical Power and Energy Systems*. 2014;54:244–254.
28. Eto JH. “Use of frequency response metrics to assess the planning and operating requirements for reliable integration of variable renewable generation,” Ernest Orlando Lawrence Berkeley National Lab., Berkeley, CA, USA, Tech. RAP. LBNL-4142E, Dec. 2011.
29. Miller NW, Shao M, Pajic S, Aquila RD. “Eastern frequency response study eastern frequency response study,” National Renewable Energy Lab., Golden, CO, USA, Tech. Rep. NREL/SR-5500-58077, May 2013 [Online]. Available: <http://www.nrel.gov/docs/fy13osti/58077.pdf>

How to cite this article: Ataee S, Bevrani H. Improvement of primary frequency control by inertial response coordination between wind and conventional power plants. *Int Trans Electr Energ Syst*. 2017;e2340. <https://doi.org/10.1002/etep.2340>